J Mol Model (2009) 15:1435–1445
DOI 10.1007/s00894-009-0509-y

ORIGINAL PAPER

Experimental and theoretical investigation of the molecular and electronic structure of 5-(4-aminophenyl)-4-(3-methyl-3-phenylcyclobutyl) thiazol-2-amine

Namık Özdemir · Muharrem Dinçer · Alaaddin Çukurovalı · Orhan Büyükgüngör

Received: 27 February 2009 / Accepted: 23 March 2009 / Published online: 8 May 2009

Abstract The title molecule, 5-(4-aminophenyl)-4-(3-methyl-3-phenylcyclobutyl)thiazol-2-amine ($C_{20}H_{21}N_3S$), was prepared and characterized by ^{1}H-NMR, ^{13}C-NMR, IR and single-crystal X-ray diffraction. The compound crystallizes in the monoclinic space group $P2_1/c$ with a= 9.4350(5) Å, b=11.2796(6) Å, c=18.4170(8) Å and β= 113.378(3)°. In addition to the molecular geometry from X-ray experiment, the molecular geometry, vibrational frequencies, gauge including atomic orbital (GIAO) ^{1}H- and ^{13}C-NMR chemical shift values and atomic charges distribution of the title compound in the ground state have been calculated using the Hartree–Fock (HF) and density functional method (DFT) (B3LYP) with 6-31G(d) basis set. To determine conformational flexibility, molecular energy profile of the title compound was obtained by semi-empirical (AM1) calculations with respect to two selected degrees of torsional freedom, which were varied from −180° to +180° in steps of 10°. Besides, frontier molecular orbitals (FMO) analysis was performed by the B3LYP/6-31G(d) method.

Keywords Ab-initio calculation · AM1 semi-empirical method · B3LYP · Conformational analysis · Hartree–Fock · NMR spectroscopy · Vibrational assignment · X-ray structure determination

Introduction

The chemistry of aminothiazoles and their derivatives has attracted the attention of chemists, since they exhibit important biological activity in medicinal chemistry [1], such as antibiotic, anti-inflammatory, anthelmintic or fungicidal properties [2–4]. 2-Aminothiazoles are known mainly as biologically active compounds with a broad range of activities and as intermediates in the synthesis of antibiotics, well known sulfa drugs, and some dyes [5, 6]. In addition, it has been shown that 3-substituted cyclobutane carboxylic acid derivatives exhibit anti-inflammatory and antidepressant activities [7], and also liquid crystal properties [8].

The gauge-including atomic orbital (GIAO) [9, 10] method is one of the most common approaches for calculating nuclear magnetic shielding tensors. It has been shown to provide results that are often more accurate than those calculated with other approaches, at the same basis set size [11].

In this study, we present results of a detailed investigation of the synthesis and structural characterization of 5-(4-aminophenyl)-4-(3-methyl-3-phenylcyclobutyl)thiazol-2-amine using single crystal X-ray, IR, NMR, and quantum chemical methods. GIAO ^{1}H- and ^{13}C-NMR chemical shifts of the title compound in the ground state have been calculated by using the Hartree–Fock (HF) and DFT (B3LYP) methods with 6–31G(d) basis set. These calcu-

Electronic supplementary material The online version of this article (doi:10.1007/s00894-009-0509-y) contains supplementary material, which is available to authorized users.

N. Özdemir (✉) · M. Dinçer · O. Büyükgüngör
Department of Physics, Faculty of Arts and Sciences,
Ondokuz Mayıs University,
55139 Kurupelit, Samsun, Turkey
e-mail: namiko@omu.edu.tr

A. Çukurovalı
Department of Chemistry,
Faculty of Arts and Sciences, Fırat University,
23119 Elazığ, Turkey

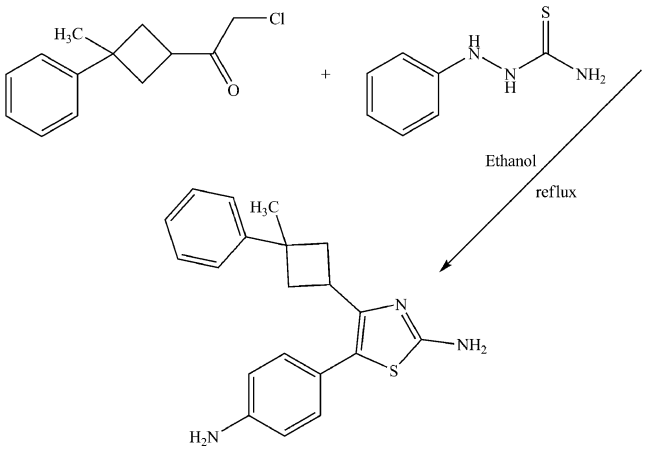

Scheme 1 Synthesis scheme of the title compound

lations are valuable for providing insight into molecular parameters and the vibration and NMR spectra.

Experimental

Synthesis

All chemicals were of reagent grade and used as commercially purchased without further purification. Melting point was determined by Gallenkamp melting point apparatus. IR spectra of the compound were recorded in the range of 4000 −450 cm^{-1} region with a Mattson 1000 FT-infrared spectrometer using KBr pellets. The ^{1}H-, and ^{13}C-nuclear magnetic resonance spectra were recorded on a Varian-Mercury 400 MHz spectrometer. Synthesis of the compound was performed with the minor modification of literature [12] method as follows (see Scheme 1). A mixture of 2.2271 g (10 mmol) 1-phenyl-1-methyl-3-(2-chloro-1-oxoethyl)cyclobutane and 4-phenylthiosemicarbazide (1.6723 g, 10 mmol) in 50 ml absolute alcohol was refluxed with continuous stirring. The course of the reaction was monitored by IR spectroscopy. The product was formed over about half an hour period. After cooling to room temperature, the solution was then made alkaline with an aqueous solution of NH_3 (5%) and light brown solid separated out. The brown colored shiny crystals which are suitable for X-ray analysis was obtained by the crystallization from ethanol (yield 81%, m.p. 528 K). Characteristic ^{1}H NMR (DMSO-d_6, δ ppm): 1.40 (s, 3H, CH_3), 2.27 (dd, j_1=8.4, j_2=10.3, 2H, –CH_2–), 2.60 (m, 2H, –CH_2–), 3.58 (q, j=9.1 Hz, 1H, >CH–), 5.20 (s, 2H, –NH_2), 6.60 (d, j=8.05 Hz, 2H, aromatics), 6.79 (s, 2H, –NH_2), 6.95 (d, j=8.05, 2H, aromatics), 7.12-7.14 (m, 3H, aromatics), 7.28 (t, j=7.68 Hz, 2H, aromatics); Characteristic ^{13}C NMR (DMSO-d_6, δ ppm): 165.78 (C1), 114.67 (C2), 153.30 (C3), 28.80 (C4), 41.07 (C5), 38.87 (C6), 30.80 (C8), 148.42 (C9), 120.34 (C10), 130.19 (C11), 125.32 (C12), 125.80 (C15), 128.81 (C16), 119.60 (C17), 148.06 (C18).

Crystal data for the title compound

CCDC 676830, $C_{20}H_{21}N_3S$, M_w=335.46, monoclinic, space group $P2_1/c$; Z=4, a=9.4350(5), b=11.2796(6), c=18.4170(8) Å, α=90, β=113.378(3), γ=90°; V=1799.09 (16) $Å^3$, $F(000)$=712, D_x=1.238 g/cm^3. Full crystallographic data are available as supplementary material.

Computational procedure

The molecular structure of the title compound in the ground state (*in vacuo*) is optimized by Hartree–Fock (HF) and

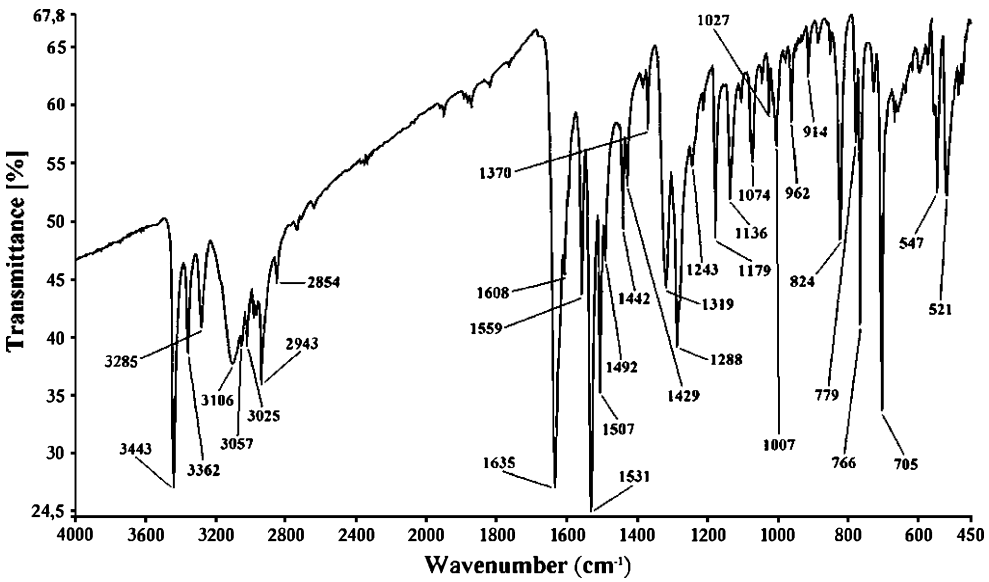

Fig. 1 FT-IR spectrum of the title compound

Table 1 Comparison of the observed and calculated vibrational spectra of the title compound

Assignments	Experimental IR with KBr (cm^{-1})	Calculated (cm^{-1}) (6-31G(d))			
		HF		B3LYP	
		Scaled freq.	I (km/mol)	Scaled freq.	I (km/mol)
ν_{as} N–H_2	–	3489	38.36	3512	21.62
ν_{as} N–H_2	3443	3474	14.52	3508	8.77
ν_{s} N–H_2	–	3389	55.46	3412	20.07
ν_{s} N–H_2	3362	3386	27.85	3409	38.87
ν_{s} C–H (aromatic)	–	3021	29.53	3082	23.08
ν_{s} C–H (aromatic)	3106	3017	6.09	3074	14.09
ν_{as} C–H (aromatic)	–	3014	22.54	3070	45.89
ν_{as} C–H (aromatic)	–	3011	54.73	3064	15.49
ν_{as} C–H (aromatic)	3057	3004	23.87	3052	27.63
ν_{as} C–H (aromatic)	3025	2988	7.94	3050	8.80
ν C–H + ν_{as} C–H_2	–	2951	49.09	3017	28.82
ν C–H + ν_{as} C–H_2	–	2941	14.11	3007	14.97
ν_{as} C–H_3	2943	2915	30.42	2990	20.54
ν C–H + ν_{as} C–H_3	–	2912	56.22	2989	29.07
ν_{s} C–H_2	–	2884	19.94	2949	17.85
ν_{s} C–H_2	–	2877	49.68	2940	38.79
ν_{s} C–H_3	2854	2856	28.59	2921	24.32
α NH_2	–	1646	150.28	1630	145.50
α NH_2	1635	1628	253.77	1608	219.22
ν C–C (aromatic) + α NH_2	–	1624	2.27	1607	22.54
ν C–C (aromatic)	1608	1617	11.42	1599	12.06
ν C=C	1559	1602	81.44	1542	75.23
ν C=N	1531	1547	237.01	1522	191.70
ν C–C (aromatic)	1507	1508	86.01	1497	47.77
ν C–C (aromatic)	1492	1494	16.07	1487	13.31
α CH_3	–	1465	1.41	1470	0.09
α CH_2	1442	1451	2.32	1442	2.23
γ CH (aromatic)	–	1438	7.73	1435	5.01
γ CH (aromatic)	1429	1421	2.60	1421	0.80
ω CH_3	1370	1394	3.00	1379	2.60
γ CH	–	1360	3.51	1336	1.57
ν C–N	1319	1321	120.52	1311	53.63
γ CH (aromatic)	–	1310	20.22	1289	1.16
ν H_3CC–C(aromatic)	–	1307	48.56	1284	82.12
γ CH + ν C–CH	1288	1289	27.57	1276	13.89
ν C–CH_3 + β CH_2	–	1258	6.21	–	–
ν C–NH_2	1243	1251	99.06	1273	86.06
ν SC–C	–	1222	10.08	1225	6.31
γ CH+ω CH_2	–	1189	2.13	1180	0.45
γ CH (aromatic)	1179	1165	35.37	1172	30.20
ν HC–CH_2	1136	1137	24.02	1126	22.67
γ CH (aromatic)	1074	1080	15.51	1121	13.38
ω CH_3	1027	1074	18.75	1067	16.38
δ CH (aromatic)	1007	965	5.70	952	0.32
θ (aromatic)	962	941	12.71	939	20.12

Table 1 (continued)

Assignments	Experimental IR with KBr (cm^{-1})	Calculated (cm^{-1}) (6-31G(d))			
		HF		B3LYP	
		Scaled freq.	I (km/mol)	Scaled freq.	I (km/mol)
δ CH (aromatic)	914	925	3.83	920	2.34
ω CH (aromatic)	824	837	88.20	810	34.87
θ (aromatic)	779	801	3.61	662	40.57
ω NH_2	766	669	98.72	647	76.95
ω NH_2	705	644	182.24	627	144.73
ω NH_2	547	619	240.58	589	336.97
ω NH_2	521	533	145.28	533	178.96

ν, stretching; β, bending; α, scissoring; γ , rocking; ω, wagging; δ, twisting; θ, ring breathing; s, symmetric; as, asymmetric

DFT(B3LYP) [13, 14] with the 6-31G(d) [15] basis set. For modeling, the initial guess of the title compound was first obtained from the X-ray coordinates. Then, vibrational frequencies for the optimized molecular structures of the title compound are calculated with these methods and then scaled by 0.8929 and 0.9613 [16], respectively. The geometry of the title compound, together with that of tetramethylsilane (TMS) is fully optimized. ^{1}H- and ^{13}C-NMR chemical shifts are calculated within GIAO approach [9, 10] applying the same methods and the basis set as that used for geometry optimization. The ^{1}H- and ^{13}C-NMR chemical shifts are converted to the TMS scale by subtracting the calculated absolute chemical shielding of TMS whose values are 32.90 and 202.14 ppm for HF/6-31G(d), and 32.17 and 190.11 ppm for B3LYP/6-31G(d), respectively. Molecular geometry is restricted, and all the calculations are performed without specifying any symmetry for the title molecule by using GaussView Molecular Visualization Program [17, 18] and Gaussian 03 Program package [19]. The effect of solvent on the theoretical NMR parameters was included using the default model provided by Gaussian 03. Dimethylsulfoxide (DMSO) was used as solvent. To identify low energy conformations, two selected degrees of torsional freedom, *T*(S1–C2–C15–C16) and *T* (C5–C6–C9–C10), were varied from −180° to +180° in steps of 10°, and the molecular energy profiles were obtained at the semi-empirical AM1 level.

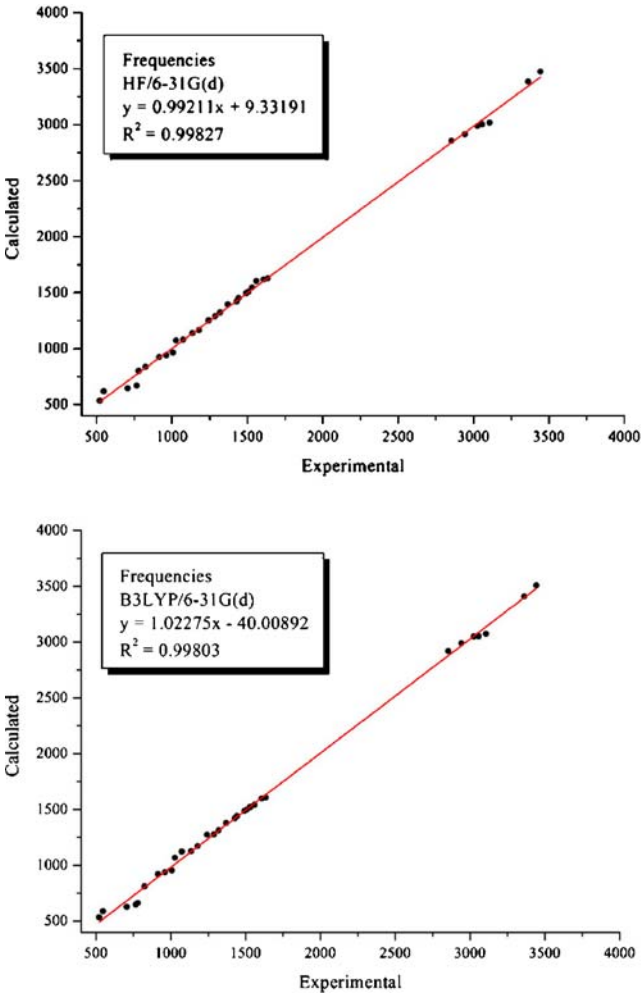

Fig. 2 Correlation graphics of calculated and experimental frequencies of the title compound

Results and discussion

IR spectroscopy

FT-IR spectra are obtained in KBr discs using a Mattson 1000 FT-IR spectrometer, and shown in Fig. 1. The band assigned to ν(C=S) vibration of thiosemicarbazide observed at 966 cm^{-1} disappeared in IR spectrum of thiazol compound because of the formation of thioether (C−S−C). In addition, the absence of any band ν(C=O) in the 1800-1700 cm^{-1} region of the IR spectrum of the compound signify that carbonyl group of 1-phenyl-1-methyl-3-(2-

Table 2 Theoretical and experimental ^{1}H and ^{13}C isotropic chemical shifts (with respect to TMS, all values in ppm) for the title compound

Atom	Experimental (ppm) (DMSO-d_6)	Calculated (ppm) (6-31G(d))	
		HF	B3LYP
C1	165.78	182.01	161.99
C2	114.67	122.82	127.25
C3	153.30	150.28	142.26
C4	28.80	28.00	30.76
C5	41.07	38.89	42.27
C6	38.87	36.13	41.69
C7	41.07	37.81	41.40
C8	30.80	31.96	31.75
C9	148.42	154.07	147.18
C10	120.34	126.62	118.85
C11	130.19	129.92	121.57
C12	125.32	126.08	118.78
C13	130.19	129.93	121.55
C14	120.34	126.72	118.93
C15	125.80	120.40	115.47
C16	128.81	135.42	124.78
C17	119.60	113.86	108.22
C18	148.06	151.56	140.09
C19	119.60	113.33	107.62
C20	128.81	136.30	124.34
H1	6.79	4.74*	4.15*
H3	5.20	3.73*	3.31*
H4	3.58	3.59	3.42
H5	2.27	2.91*	2.62*
H7	2.60	2.79*	2.54*
H8	1.40	1.70*	1.39*
H10	7.14	7.93	7.24
H11	7.12	8.13	7.39
H12	7.28	7.96	7.27
H13	7.12	8.13	7.42
H14	7.14	7.89	7.22
H16	6.60	8.00	7.04
H17	6.95	7.36	6.60
H19	6.95	7.37	6.58
H20	6.60	7.95	6.98

* Average

chloro-1-oxoethyl)cyclobutane reacted with amino group of thiosemicarbazide. The bands at 3443, 3362 and 1635 cm^{-1} observed in the IR spectrum are assigned to asymmetric, symmetric stretchings and N−H intra-planar bending of NH_2 group.

It is well known, that the calculated HF and DFT 'raw' or 'non-scale' harmonic frequencies could significantly overestimate experimental values due to lack of electron correlation, insufficient basis sets and anharmonicity. Much effort has been devoted to accurately reproducing experimental frequencies in theoretical calculations. The Hartree–Fock calculated results are usually more overestimated than the corresponding DFT ones [20]. To compare these, we have calculated the theoretical vibrational spectra of the title compound using both HF and B3LYP method with 6-31G(d) basis set. Frequency calculations at the same levels of theory revealed no imaginary frequencies, indicating that an optimal geometry at these levels of approximation was found for the title compound. We have compared our calculation of the title compound with their experimental results. Theoretical and experimental results of the title compound are shown in Table 1. The vibrational bands assignments have been made by using Gauss-View Molecular Visualization program [17]. To make comparison with experiment, we present correlation graphics in Fig. 2 based on the calculations. As we can seen from correlation graphic in Fig. 2 experimental fundamentals are in better agreement with the scaled fundamentals and are found to have a better correlation for HF than B3LYP.

As can be seen from Table 1, the NH_2 asymmetric and symmetric stretch bands have been calculated at 3474–3386 cm^{-1} for HF and 3508–3409 cm^{-1} for B3LYP with using 6-31G(d) basis set. The experimental C=C and C=N stretch bands were observed at 1559 and 1531 cm^{-1}, that have been calculated with HF and B3LYP at 1602–1547 and 1542–1522 cm^{-1}, respectively. As can be seen from Table 1, there is also good agreement between experimental and theoretical vibration data for the others.

NMR spectroscopy

GIAO ^{1}H and ^{13}C chemical shift calculations have been carried out using the HF and B3LYP methods with 6–31G (d) basis set for the optimized geometry. The results of these calculations are tabulated in Table 2. Since experi-

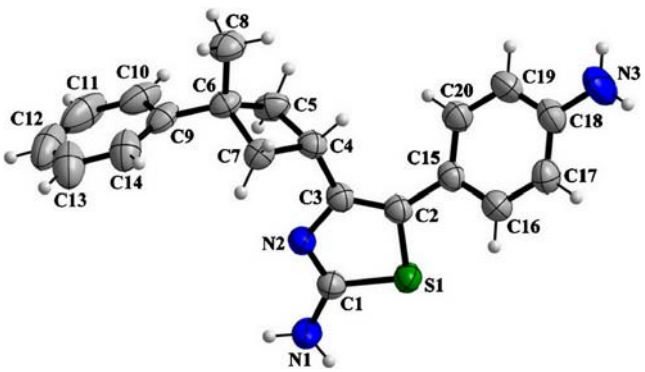

Fig. 3 The molecular structure of the title molecule, showing the atom-numbering scheme. Displacement ellipsoids are drawn at the 50% probability level and H atoms are shown as small spheres of arbitrary radii

Table 3 Hydrogen bonding geometry (Å, °) for the title compound

D—H···A	D—H	H···A	D···A	D—H···A
N1—H1A···N2^{i}	0.86	2.15	2.994 (2)	168
N1—H1B···Cg1^{i}	0.86	2.37	3.217 (2)	171
C14—H14···Cg2^{ii}	0.93	2.68	3.499 (2)	147

Symmetry codes: (i) 1 − *x*, 1 − *y*, 1 − *z*; (ii) − *x*, −0.5 + *y*, +0.5 − *z*. Cg1: the centroid of the C9 − C14 ring, Cg2: the centroid of the C15 − C20 ring

mental ^{1}H chemical shift values were not available for individual hydrogen, we have presented the average values for NH_2, CH_2 and CH_3 hydrogen atoms. The signals assigned hydrazinic NH of the thiosemicarbazide in the 9-12 ppm range disappear in the ^{1}H-NMR spectrum of the thiazol compound [21, 22]. The singlets observed at 5.20 and 6.79 ppm are assigned to N(3)H_2 and N(1)H_2 groups, respectively, that have been calculated with HF and B3LYP at 3.73–4.74 and 3.31–4.15 ppm. The -CH_2- signals of the cyclobutane are observed at 2.27 and 2.60 ppm. The C-H signals belonging to p-aminophenyl group are shielded at 6.60 and 6.95 ppm. However, the C-H signals of phenyl adjacent to the cyclobutane are deshielded at 7.12-7.14 (3H) and 7.28 (2H) ppm. The singlet signal of the methyl group is observed at 1.40 ppm.

^{13}C-NMR spectra of the thiazol compound show the signal at 165.78 ppm due to C atom next to N(1)H_2. This signal has been calculated as 182.01 ppm for HF and 161.99 ppm for B3LYP. The signals at 114.67 and 153.30 ppm are assigned to C atoms next to sulfur and nitrogen atom of thiazol ring, respectively. While the C atoms of methylene group belonging to the cyclobutane ring are observed at 41.07 ppm, methine C atom appeared at 28.80 ppm. The signal at 38.87 ppm is related to the last C atom of the cyclobutan ring.

Comparing calculational and the experimental data, we studied the relativity between the calculation and the experiments, and obtained that the linear function formula is y= 1.02406x – 0.4658 for HF; where R^2 is 0.99547, and y= 0.95535x+0.67306 for B3LYP; where R^2 is 0.99493. According to these results, it is seen that, the results of HF method have shown better fit to experimental ones than B3LYP in evaluating ^{1}H and ^{13}C chemical shifts.

Description of the structure

The title compound, a DIAMOND [23] view of which is shown in Fig. 3, crystallizes in the monoclinic space group $P2_1/c$ with four molecules in the unit cell. The asymmetric unit in the crystal structure contains only one molecule.

The title molecule is composed of a central thiazole ring, with an amino group connected to the 2-position of the ring, a (3-methyl-3-phenyl)cyclobutyl group in the 4-position, and a *p*-aminophenyl group in the 5-position. The thiazole ring is planar with a maximum deviation of -0.0055(10) Å for atom N2. In the crystal structure, the benzene ring and 5-(4-aminophenyl)thiazol-2-amine group are in *cis* positions with respect to the cyclobutane ring. The dihedral angles between the thiazole plane *A* (S1/N2/C1−C3), the benzene plane *B* (C9−C14), the cyclobutane plane *C* (C4−C7) and the other benzene plane *D* (C15−C20) are 88.68(6)° (*A*/*B*), 83.60(8)° (*A*/*C*), 43.75(4)° (*A*/*D*), 45.42(10)° (*B*/*C*), 47.99(8)° (*B*/*D*) and 67.89(8)° (*C*/*D*).

Although close to being planar, the cyclobutane ring is puckered. The C7/C4/C5 plane forms a dihedral angle of 18.92(15)° with the C5/C6/C7 plane. This value is smaller than those in the literatures; 23.5 [24], 25.74(6) [25], and

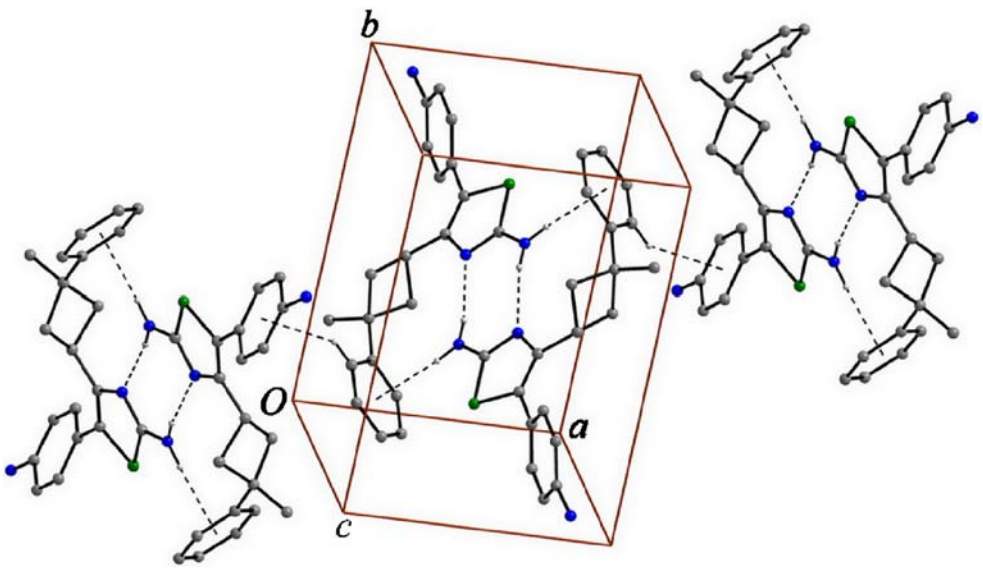

Fig. 4 Part of the crystal structure of the title molecule, showing the formation of a chain of centrosymmetric $R_2^2(8)$ dimers. For clarity, only H atoms involved in hydrogen bonding have been included

Table 4 Optimized and experimental geometries of the title compound in the ground state

Parameters	Experimental	Calculated (6-31G(d))	
		HF	B3LYP
Bond lengths (Å)			
S1–C1	1.7338(17)	1.7408	1.7632
S1–C2	1.7503(16)	1.7625	1.7754
N1–C1	1.348(2)	1.3709	1.3813
N2–C1	1.300(2)	1.2743	1.2990
N2–C3	1.3972(19)	1.3871	1.3867
N3–C18	1.388(2)	1.3938	1.3968
C2–C3	1.350(2)	1.3450	1.3742
C2–C15	1.476(2)	1.4812	1.4699
C3–C4	1.486(2)	1.4984	1.4982
C4–C5	1.542(3)	1.5478	1.5597
C4–C7	1.547(2)	1.5474	1.5580
C5–C6	1.553(2)	1.5531	1.5626
C6–C9	1.511(3)	1.5176	1.5172
C6–C8	1.527(2)	1.5354	1.5401
C6–C7	1.547(2)	1.5533	1.5628
Bond angles (°)			
C1–S1–C2	89.27(8)	88.5542	88.5806
C1–N2–C3	111.05(14)	111.5356	111.6035
N2–C1–N1	124.51(16)	123.7216	123.8191
N2–C1–S1	114.67(12)	115.0842	114.8993
N1–C1–S1	120.82(13)	121.1336	121.1626
C3–C2–C15	131.91(15)	130.7155	131.0501
C3–C2–S1	109.39(12)	108.7592	108.7471
C15–C2–S1	118.63(12)	120.5221	120.1985
C2–C3–N2	115.62(14)	116.0591	116.1565
C2–C3–C4	127.30(14)	126.2723	126.1719
N2–C3–C4	117.07(14)	117.6675	117.6625
C3–C4–C5	117.22(14)	118.2661	118.2830
C3–C4–C7	118.19(14)	118.1296	118.0213
C5–C4–C7	88.24(13)	88.0340	88.0082
C4–C5–C6	90.37(12)	89.2588	89.3551
C9–C6–C8	110.38(14)	109.6037	109.7499
C9–C6–C7	116.31(14)	117.3868	117.2575
C8–C6–C7	112.42(14)	111.7274	111.7055
C9–C6–C5	115.71(14)	117.3034	117.2668
C8–C6–C5	112.62(15)	111.7140	111.6233
C7–C6–C5	87.83(12)	87.6341	87.7375
C4–C7–C6	90.36(12)	89.2672	89.4096
C19–C18–N3	121.02(19)	120.8043	120.9625
C17–C18–N3	121.0(2)	120.7296	120.8606
Torsion angles (°)			
S1–C2–C15–C20	137.35(15)	116.4468	133.0936
S1–C2–C15–C16	−42.30(19)	−62.8068	−46.0387
C2–C3–C4–C5	121.19(18)	124.8009	122.1078
C2–C3–C4–C7	−135.14(17)	−131.1187	−133.9088
C4–C3–C2–C15	1.7(3)	−1.9831	−3.1613
C4–C5–C6–C9	−131.78(15)	−137.8404	−137.2529
C4–C7–C6–C9	131.18(14)	137.7695	137.2812
C5–C6–C9–C10	−38.8(2)	−40.4267	−39.7911

19.26(17)° [26]. However, when the bond lengths and angles of the cylobutane ring in the title compound are compared with these, it is seen that there are no significant differences.

There are two obviously different C−N bond distances in the thiazole ring, *viz*. N2−C1 and N2−C3. The C2−C3 bond distance is 1.350(2) Å, characterizing a C=C double bond. The N1−C1 bond distance [1.348(2) Å] is shorter than the single bond N2−C3 [1.3972(19) Å], but longer than that of the double bond N2−C1 [1.300(2) Å], which can be attributed to the conjugation of the electrons of atom N1 with atoms C1 and N2. In addition, the S1−C1 bond distance [1.7338(17) Å], which is shorter than the S1−C2 bond [1.7503(16) Å], being both much shorter than the lower-quartile value [1.809 Å;[27]] for single bonds between three-connected C and two-connected S atoms, arises from the conjugation of the electrons of atom S1 with atoms C1 and N2.

The crystal structure does not exhibit intramolecular or π–π stacking (face-to-face) interactions. There are, however, one N−H···N and two X−H···Cg(π-ring) (edge-to-face) intermolecular interactions, details of which are given in Table 3. Amino atom N1 in the molecule at (*x*, *y*, *z*) acts as hydrogen-bond donor, *via* atom H1A, to ring atom N2 in the molecule at (1−*x*, 1−*y*, 1−*z*), so generating by inversion a centrosymmetric dimer, centered at (1/2, 1/2, 1/2) and characterized by an $R_2^2(8)$ motif [28] (Fig. 4). The same amino atom N1 at (*x*, *y*, *z*) forms a N—H···Cg(π-ring) contact, this time *via* atom H1B, with the centroid of the C9−C14 ring [*fractional centroid coordinates:* 0.8017(2), 0.8569(3), 0.6145(2)] of the molecule at (1 − *x*, 1 − *y*, 1 − *z*). In addition, atom C14 at (*x*, *y*, *z*) forms a C—H···Cg(π-ring) contact, *via* atom H14, with the centroid of the C15−C20 ring [*fractional centroid coordinates:* -0.2799(3), 0.3161(2), 0.3606(2)] of the molecule at (−*x*, −0.5 + *y*, +0.5 − *z*), which links the $R_2^2(8)$ dimers into a molecular chain.

Theoretical structures

Some selected geometric parameters experimentally obtained and theoretically calculated by HF and B3LYP with 6-31G(d) as the basis set are listed in Table 4. When

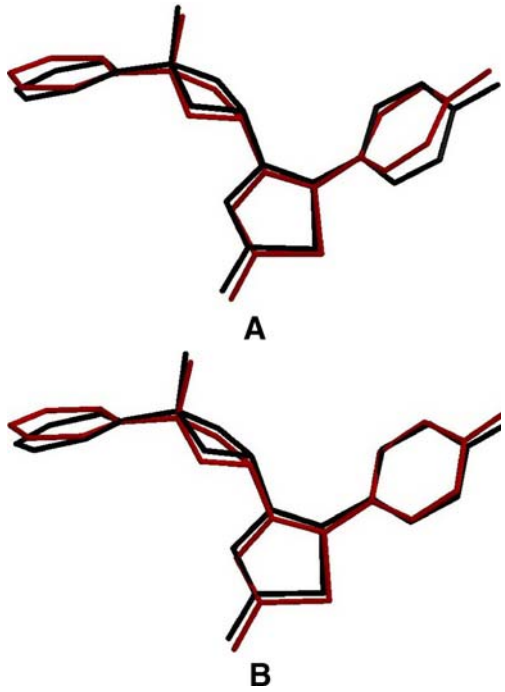

Fig. 5 Atom-by-atom superimposition of the structures calculated (red) [A = HF; B = B3LYP] over the X-ray structure (black) for the title compound. Hydrogen atoms omitted for clarity. The RMS overlay error of 0.308 and 0.244 Å does not include hydrogen atoms

the X-ray structure of the title compound is compared with its optimized counterparts (see Fig. 5), conformational discrepancies are observed between them. The dihedral angles between *A, B, C* and *D* planes are calculated at 87.45° (*A*/*B*), 86.56° (*A*/*C*), 62.69° (*A*/*D*), 35.89° (*B*/*C*), 38.02° (*B*/*D*) and 67.25° (*C*/*D*) for HF, and at 86.28° (*A*/*B*), 83.50° (*A*/*C*), 45.89° (*A*/*D*), 36.38° (*B*/*C*), 47.55° (*B*/*D*) and 67.59° (*C*/*D*) for B3LYP. According to X-ray study, dihedral angle between the C7/C4/C5 and C5/C6/C7 planes is 18.92(15)°, whereas the dihedral angle has been calculated at 25.53° for HF and at 24.82° for B3LYP.

For the optimized geometric parameters, various methods including HF method estimates some bond lengths well to some extent [29–31]. We noted that the experimental results belong to solid phase and theoretical calculations belong to gaseous phase. In the solid state, the existence of the crystal field along with the intermolecular interactions have connected the molecules together, which result in the differences of bond parameters between the calculated and experimental values. It is well known that DFT optimized bond lengths are usually longer and more accurate than HF, due to inclusion of electron correlation. However, according to our calculations, HF method correlates well for the bond length compared with the other method (Table 4). The largest difference between experimental and calculated HF bond length is about 0.026 Å. The B3LYP method leads to geometric parameters (angles), which are much closer to experimental data. This pattern was not found for bond length, as can be seen from Table 4, whereas in the case of B3LYP method, the biggest difference between calculated and experimental values of bond lengths was 0.033 Å. The bond angles provided by B3LYP method is the closest to the experimental values (Table 4). The largest difference is about 1.57° in the case of B3LYP method, while this difference is 1.90° for HF. The same trend was also observed in torsion angles. The largest differences are 20.9° and 6.1° for HF and B3LYP, respectively. As a result, the optimized bond lengths obtained by HF method, and bond angles and torsion angles by DFT (B3LYP) method show the best agreement with the experimental values.

Based on HF/6-31G(d) and B3LYP/6-31G(d) optimized geometry, the total energy of the title compound has been calculated by these two methods, which are −1330.434223 and −1337.204818 a.u., respectively. In order to define the preferential position of the aminobenzene fragment with respect to thiazole ring, and the preferential position of the

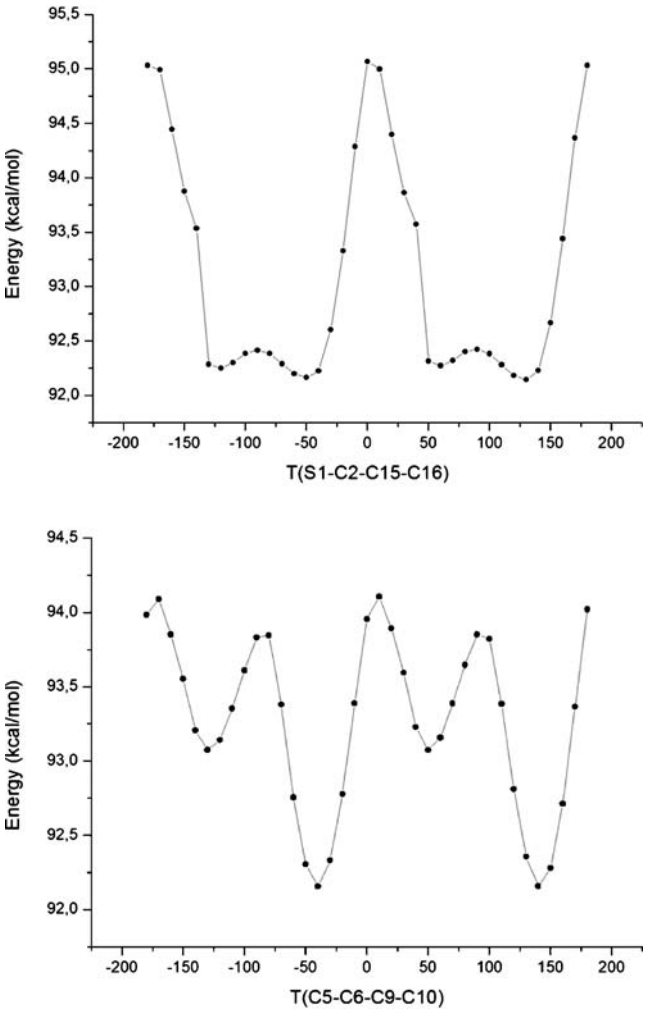

Fig. 6 Molecular energy profiles of the optimized counterpart of the title compound against the selected degrees of torsional freedom

Table 5 Atomic charges (*e*) of the title compound at HF/6-31G(d) and B3LYP/6-31G(d) levels

Atom	HF/6-31G(d)		B3LYP/6-31G(d)	
	Mulliken atomic charges	NPA atomic charges	Mulliken atomic charges	NPA atomic charges
S1	0.246	0.349	0.184	0.350
N1	−0.882	−0.892	−0.750	−0.846
N2	−0.589	−0.623	−0.502	−0.534
N3	−0.892	−0.877	−0.788	−0.832
C1	0.369	0.358	0.285	0.250
C2	−0.342	−0.266	−0.287	−0.234
C3	0.345	0.206	0.327	0.157
C4	−0.234	−0.257	−0.182	−0.273
C5	−0.312	−0.402	−0.287	−0.432
C6	−0.063	−0.062	0.015	−0.067
C7	−0.311	−0.401	−0.286	−0.431
C8	−0.456	−0.617	−0.453	−0.661
C9	0.043	−0.022	0.146	−0.027
C10	−0.223	−0.228	−0.181	−0.230
C11	−0.194	−0.214	−0.131	−0.228
C12	−0.209	−0.241	−0.131	−0.244
C13	−0.194	−0.213	−0.131	−0.228
C14	−0.223	−0.227	−0.180	−0.229
C15	−0.015	−0.136	0.125	−0.113
C16	−0.188	−0.157	−0.186	−0.197
C17	−0.255	−0.296	−0.176	−0.277
C18	0.303	0.231	0.316	0.171
C19	−0.257	−0.298	−0.181	−0.279
C20	−0.182	−0.157	−0.179	−0.198

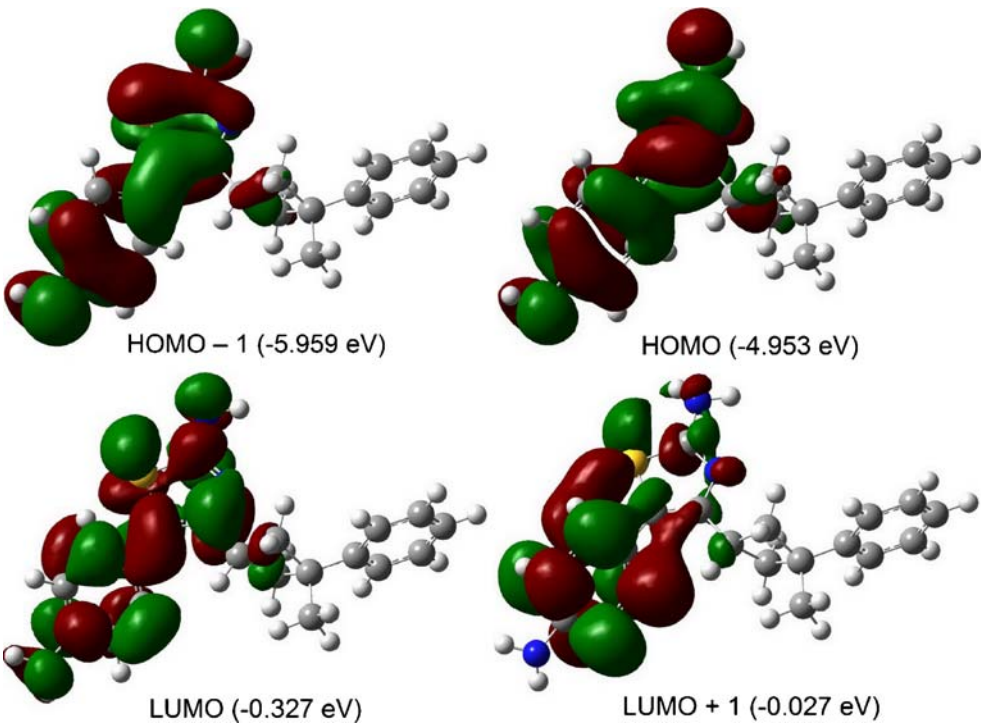

Fig. 7 Molecular orbital surfaces and energy levels given in parentheses for the *HOMO* – 1, *HOMO*, *LUMO* and *LUMO* + 1 of the title compound computed at B3LYP/6-31G(d) level

benzene ring with respect to the cyclobutane ring, respectively, a preliminary search of low energy structures was performed using AM1 computations as a function of the selected degrees of torsional freedom *T*(S1–C2–C15–C16) and *T*(C5–C6–C9–C10). The respective values of the selected degrees of torsional freedom, *T*(S1–C2–C15–C16) and *T*(C5–C6–C9–C10), are -42.30(19) and -38.8 (2)° in X-ray structure, whereas the corresponding values in optimized geometries are -62.8068 and -40.4267° for HF, and -46.0387 and -39.7911° for B3LYP. Molecular energy profiles with respect to rotations about the selected torsion angles are presented in Fig. 6. According to the results, the low energy domains for *T*(S1–C2–C15–C16) are located at -50 and 130° having energy of 92.165 and 92.142 kcal mol^{-1}, respectively, while they are located at -40 and 140° having energy of 92.156 and 92.158 kcal mol^{-1}, respectively, for *T*(C5–C6–C9–C10). Energy difference between the most favorable and unfavorable conformer, which arises from rotational potential barrier calculated with respect to the two selected torsion angles, is calculated as 2.926 kcal mol^{-1} when both selected degrees of torsional freedom are considered.

The molecular energy can be divided into bonded and non-bonded contributions. The bonded energy is considered to be independent of torsional angle changes and therefore vanished when relative conformer energies are calculated. The non-bonded energy is further separated into torsional steric and electrostatic terms [32]. Since the title compound contains no intramolecular hydrogen bond, it can be deduced from the computational results that the most stable conformer of the title compound is principally determined by the non-bonded torsional energy term affected by packing of the molecules.

The Mulliken atomic charges and natural population analysis (NPA) atomic charges for the non-H atoms of the title compound calculated at HF/6-31G(d) and B3LYP/6-31G(d) levels are presented in Table 5. The calculated results show that the two amino N atoms have bigger negative charges along with their suitable spatial configuration, which result in that they are the potential sites to react with the metallic cores. Namely, the title compound can act as multidentate ligand to bind one or two metal centers, so resulting in interesting metal complexes with different coordination geometries.

Figure 7 shows the distributions and energy levels of the *HOMO* − 1, *HOMO*, *LUMO* and *LUMO* + 1 orbitals computed at the B3LYP/6-31G(d) level for the title compound. Both the highest occupied molecular orbitals (*HOMO*s) and the lowest-lying unoccupied molecular orbitals (*LUMO*s) are mainly localized on the aminobenzene and aminothiazole fragments indicating that the *HOMO-LUMO* are mostly the π-antibonding type orbitals, and are perpendicularly oriented to each other. The value of the energy separation between the *HOMO* and *LUMO* is 4.626 eV and this large energy gap indicates that the title structure is very stable.

Conclusions

As a result, X-ray structure is slightly different from its optimized counterparts, and the crystal structure is stabilized by N−H···N type hydrogen bonds and edge-to-face interactions. Crystal packing of the title compound is dominated only by intermolecular interactions formed during preparation or crystallization. These hydrogen bonds supply leading contribution to the stability and to the order of the crystal structure, and are presumably responsible for the discrepancies between the X-ray and optimized structures of the title compound. For the geometric parameters, the results of B3LYP method has shown a better fit to experimental ones than HF in evaluating geometrical parameters. However, the HF method seems to be more appropriate than B3LYP method for the calculation of vibrational frequencies and chemical shifts.

Acknowledgments This study was supported financially by the Research Centre of Ondokuz Mayıs University (Project No: F-425).

References

1. Barone R, Chanon M, Gallo R (1979) Aminothiazoles and their derivatives: The chemistry of heterocyclic compounds, vol 34. Interscience Publishers, Wiley, New York, pp 9–366
2. Crews P, Kakou Y, Quinoa E (1988) J Am Chem Soc 110:4365–4368
3. Shinagawa H, Yamaga H, Houchigai H, Sumita Y, Sunagawa M (1997) Bioorg Med Chem 5:601–621
4. Shivarama Holla B, Malini KV, Sooryanarayana Rao B, Sarojini BK, Suchetha Kumari N (2003) Eur J Med Chem 38:313–318
5. Nam G, Lee JC, Chi DY, Kim J-H (1990) Bull Korean Chem Soc 11:383–386
6. Ibatullin UG, Petrushina TF, Leitis LY, Minibaev IZ, Logvin BO (1993) Khim Geterotsikl Soedin 715 (USSR); Chem Abstr, 1994, 120, 1145
7. Dehmlow EV, Schmidt S (1990) Liebigs Ann Chem 5:411–414
8. Coghi L, Lanfredi AMM, Tiripicchio A (1976) J Chem Soc Perkin Trans 2:1808–1810
9. Ditchfield R (1972) J Chem Phys 56:5688–5691
10. Wolinski K, Hinton JF, Pulay P (1990) J Am Chem Soc 112:8251–8260
11. Cheeseman JR, Trucks GW, Keith TA, Frisch MJ (1996) J Chem Phys 104:5497–5509
12. Lee BW, Lee SD (2000) Tetrahedron Lett 41:3883–3886
13. Lee C, Yang W, Parr RG (1988) Phys Rev B 37:785–789
14. Becke AD (1993) J Chem Phys 98:5648–5652
15. Ditchfield R, Hehre WJ, Pople JA (1971) J Chem Phys 54:724–728
16. Foresman JB, Frisch A (1996) Exploring chemistry with electronic structure methods, 2nd edn. Gaussian Inc, Pittsburgh
17. Dennington R II, Keith T, Millam J (2007) GaussView, Version 4.1.2. Semichem Inc, Shawnee Mission, KS

18. Frisch A, Dennington R II, Keith T, Millam J, Nielsen AB, Holder AJ, Hiscocks J (2007) GaussView Reference, Version 4.0. Gaussian Inc, Pittsburgh
19. Frisch MJ, Trucks GW, Schlegel HB, Scuseria GE, Robb MA, Cheeseman JR, Montgomery JA Jr, Vreven T, Kudin KN, Burant JC, Millam JM, Iyengar SS, Tomasi J, Barone V, Mennucci B, Cossi M, Scalmani G, Rega N, Petersson GA, Nakatsuji H, Hada M, Ehara M, Toyota K, Fukuda R, Hasegawa J, Ishida M, Nakajima T, Honda Y, Kitao O, Nakai H, Klene M, Li X, Knox JE, Hratchian HP, Cross JB, Bakken V, Adamo C, Jaramillo J, Gomperts R, Stratmann RE, Yazyev O, Austin AJ, Cammi R, Pomelli C, Ochterski JW, Ayala PY, Morokuma K, Voth GA, Salvador P, Dannenberg JJ, Zakrzewski VG, Dapprich S, Daniels AD, Strain MC, Farkas O, Malick DK, Rabuck AD, Raghavachari K, Foresman JB, Ortiz JV, Cui Q, Baboul AG, Clifford S, Cioslowski J, Stefanov BB, Liu G, Liashenko A, Piskorz P, Komaromi I, Martin RL, Fox DJ, Keith T, Al-Laham MA, Peng CY, Nanayakkara A, Challacombe M, Gill PMW, Johnson B, Chen W, Wong MW, Gonzalez C, Pople JA (2004) Gaussian 03, Revision E.01. Gaussian Inc, Wallingford, CT
20. Zhou W, Lu J, Zhang Z, Zhang Y, Cao Y, Lu L, Yang X (2004) Vibr Spectrosc 34:199–204
21. Yılmaz İ, Çukurovalı A (2003) Heteroatom Chem 14:617–621
22. Bal-Demirci T (2008) Polyhedron 27:440–446
23. Brandenburg K (2006) DIAMOND, Demonstration version 3.1.e. Crystal Impact GbR, Bonn, Germany
24. Swenson DC, Yamamoto M, Burton DJ (1997) Acta Crystallogr A C53:1445–1447
25. Çukurovalı A, Özdemir N, Yılmaz İ, Dinçer M (2005) Acta Crystallogr E61:o1754–o1756
26. Dinçer M, Özdemir N, Yılmaz İ, Çukurovalı A, Büyükgüngör O (2004) Acta Crystallogr C60:o674–o676
27. Allen FH, Kennard O, Watson DG, Brammer L, Orpen AG, Taylor R (1987) J Chem Soc Perkin Trans 2:1–19
28. Bernstein J, Davis RE, Shimoni L, Chang N-L (1995) Angew Chem Int Ed Engl 34:1555–1573
29. Wheeless CJM, Zou X, Liu R (1995) J Phys Chem 99(33):12488–12492
30. Lee SY, Boo BH (1996) J Phys Chem 100:15073–15078
31. Atalay Y, Avcı D, Başoğlu A, Okur İ (2005) J Mol Struct Theochem 713:21–26
32. Weiqun Z, Baolong L, Yang C, Yong Z, Xujie LLY (2005) J Mol Struct Theochem 715:117–124